Mechanism, kinetics and modelling of the inverse-microsuspension homopolymerization of acrylamide

D. Hunkeler, A. E. Hamielec and W. Baade
Institute for Polymer Production Technology, and Department of Chemical Engineering, McMaster University, Hamilton, Ontario, Canada
(Received 1 March 1988; accepted 7 June 1988)

The polymerization of water-soluble monomers is industrially often carried out in inverse-microsuspension or inverse emulsion. Although the kinetics of these processes have been investigated extensively over the past decade, there has been no mechanism proposed which can predict rates and molecular weights. In this paper a general mechanism is developed for inverse-microsuspension polymerization in paraffinic media with oil-soluble initiators. It is compared with experimental data for acrylamide polymerizations and is found to predict conversion, molecular weight and particle characteristics quite well. The mechanism consists of the initiation, propagation, transfer and termination reactions that are common to all free-radical polymerizations. It also includes three newly proposed steps: the reaction between a macroradical and an interfacial emulsifier, which has been found to dominate over the conventional bimolecular reaction; a long-chain branching reaction with terminal unsaturated carbons; and the mass transfer of primary radicals and oligoradicals between organic and aqueous phases. These have a profound effect on the kinetics, where the rate is found to depend on the initiator level to a power greater than one-half and to be inversely proportional to the surface emulsifier concentration. Owing to the importance of unimolecular termination and long-chain branching in inverse microsuspension, certain classes of emulsifier have been identified as being most suitable for the production of ultra-high-molecular-weight polymers.

(Keywords: inverse-microsuspension; inverse-emulsion; acrylamide; water-soluble polymers)

INTRODUCTION

The production of water-soluble polymers exceeds five million tons per annum. About 10% of this is synthetic polymers of which polyacrylamide, poly(acrylic acid) and their copolymers are the most important. High-molecular-weight homopolymers of acrylamide are used as pushing fluids in tertiary oil recovery, as drag reduction agents and as drilling fluids. Copolymers with various cationic monomers such as diallyldimethylammonium chloride are used for fines retention in paper making, as flocculants, and in general wherever aqueous solid–liquid separations are required. Lightly crosslinked polymers of sodium acrylate are superabsorbent and are used in many applications, perhaps the most important of which is for adult and baby diapers (nappies).

Because acrylamide is a solid at normal reaction temperatures it is usually polymerized in aqueous solutions[1-11]. The presence of organic additives such as alcohols, acetone, dimethylsulphoxide (DMSO) and tetrahydrofuran (THF) are undesirable because they reduce the rate of polymerization and the molecular weight[12,13]. Furthermore, the reaction should be performed in neutral solutions and at moderate temperatures ($<70°C$) to avoid imidization.

The polymerization of acrylamide is characterized by a very high heat generation rate and a highly viscous product, which remains on the reaction vessel and is difficult to remove. Industrially, several variations have been employed to overcome these difficulties. These include polymerizing in thin layers and on cold surfaces[14-17], the addition of a volatile organic to provide evaporative cooling[18,19] and polymerization in a reactor lined with a polyethylene bag to prevent polymer sticking to the equipment[20].

However, the polymerization of these polymers is often carried out in inverse-microsuspension or as it is more commonly called inverse-emulsion. This involves the emulsification of a water-soluble monomer, in solution, in a continuous organic phase. A water-in-oil steric stabilizer is used and the polymerization is carried out with either a water- or oil-soluble initiator, although the latter is more common.

Microsuspensions have lower viscosities, provide easier heat removal and can be used at higher monomer concentrations than the solution process. Furthermore, the inverse latices produced can be easily inverted and added to water so that water-swollen polymer particles dissolve rapidly. In contrast, polymer which has been dried experiences gel blocking when added to water.

There have been several different investigations of the kinetics of heterophase acrylamide polymerizations[21-29]. These can be divided into three categories depending on the solubility of the initiator and the chemical nature of the continuous phase. The kinetics for each of these is very different, as is shown in *Table 1*.

When water-soluble initiators are used, all components for the polymerization reside in the dispersed droplets. Each particle acts essentially as a small batch reactor and

0032-3861/89/010127-16$03.00

Table 1 Kinetics of heterophase acrylamide polymerizations

Solubility of initiator	Type of continuous phase	Rate expression	Comments
Water	Paraffinic or aromatic	$R_p \propto [M]^{1.25}[I]^{0.5}$	Kinetics are the same as for solution polymerization
Oil	Aromatic	$R_p \propto [M][I][E]^b$ $b>0$	Inverse emulsion[a]; polymerization in inverse micelles
Oil	Paraffinic	$R_p \propto [M][I]^a[E]^b$ $0.5<a<1.0$ $b<0$	Inverse microsuspension; polymerization in monomer droplets

[a] Inverse emulsions are also obtained in paraffinic media with aerosol emulsifiers

Table 2 Comparison of inverse-microsuspension and emulsion polymerizations

	Inverse microsuspension	Suspension	Emulsion
N_p	Constant throughout reaction and independent of initiator concentration	Constant throughout reaction and independent of initiator concentration	Grows during stage I; $\propto [I]^{0.4-1.0}$
d_p	$\propto$ (stirrer speed)$^{-1.3}$	$\propto$ (stirrer speed)$^{-(1.2\rightarrow1.5)}$	$\propto$ (stirrer speed)$^{0\rightarrow0.1}$
$\bar{n}$	10→80	>20	<5–10 usually
Initiation	No inverse micelles detectable; loci of initiation are monomer droplets	Loci of initiation are monomer droplets	Initiation by micelles or homogeneous nucleation
Effect of emulsifier on rate	Reduces rate	Confers stability	Increases rate by producing more particles
Species which transfer between phases	Primary radicals and oligoradicals	–	Primary radicals, oligoradicals and monomer

the kinetics are similar to those for solution polymerization. The molecular weight is lower, however, due to transfer to the hydrophilic part of the emulsifier[26,30].

When oil-soluble initiators are used with aromatic continuous phases the kinetics have been shown to resemble emulsion polymerization*[21,22] with the locus of initiation occurring in inverse micelles. However, when paraffinic oil phases are used, as is most common commercially, the locus of initiation is in the monomer droplets. This has been verified by dynamic light scattering measurements which failed to detect inverse micelles[24] and indicated a constant particle morphology throughout the reaction[31]. The polymerization therefore physically and kinetically resembles a suspension (*Table 2*), and is referred to as inverse-microsuspension, the prefix 'micro' being added beacuse the average particle size is nominally 1 μm.

There have been several investigations into the kinetics of inverse-microsuspension polymerization, most recently and extensively by Baade in 1986[32]. However, a reliable tested mechanism has still not been found which can describe the polymerization. The focus of this paper is to synthesize previous experimental results into a set of elementary reactions and to evaluate the resulting kinetic model against rate, molecular-weight and particle-size data.

EXPERIMENTAL

Aqueous solutions of acrylamide were dispersed in isoparaffinic hydrocarbons with various emulsifiers based on sorbitan esters by stirring with a propeller-type agitator to form a water-in-oil emulsion. After purging with nitrogen, the polymerization was initiated by injecting an oil-soluble azo initiator into the system. The polymerization was run in a batch mode at constant temperature.

The chemicals used were as follows: acrylamide monomer (American Cyanamide, Nalco), polymerization grade; Isopar M (Esso Chemie), an isoparaffinic mixture with a boiling range of 204–247°C as the continuous phase; sorbitan monooleate (SMO) and sorbitan monostearate (SMS) (Atlas Chemie), 99% purity, as emulsifiers; ethylenediaminetetraacetic acid (EDTA, Merck) as chelating agent to remove ion inhibitors; bortrioxide (Merck) as a buffering agent; and the initiators azobisisobutyronitrile (AIBN, Bayer AG) and azobisdimethylvaleronitrile (ADVN, Wako).

The polymerization procedure was as follows. Oil with the dissolved emulsifier was added to the water phase and stirred at 1000 rpm to produce a dispersion. During this time the system was purged with rarefied nitrogen (99.99%) to remove residual oxygen. Then approximately 5 ml of the initiator solution was injected through a silicone cap to start the polymerization. All polymerizations were isothermal with temperature control within 1°C. The reactor was a 1.3 litre batch reactor (ratio of height to diameter 3:1) with two baffles and a propeller stirrer of one-quarter diameter (15 cm) of the vessel, arranged symmetrically about the centre.

All polymerizations were carried out with equiphase ratios of water to oil. This corresponded to 570 g of aqueous phase and 430 g of organic phase.

Trace levels of oxygen, which could not be removed by purging, inhibit the reaction by consuming initiator radicals. Initially the high propensity for this reaction stops the polymerization completely. As the oxygen level depletes, propagation becomes more favourable and the polymerization commences. The rate slowly increases until all residual oxygen is consumed, at which point it reaches a maximum. In order to use the kinetic data the effect of oxygen is removed by performing a first-order correction to the S-shaped conversion–time data, as is shown in *Figure 1*.

In general the conversion was determined by

* Using aerosol emulsifiers also results in inverse micelles[31]

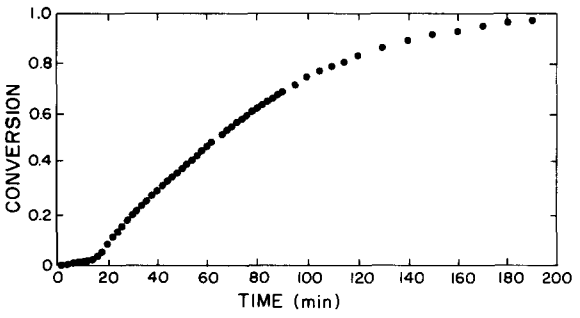

Figure 1 Experimental conversion–time data showing an induction time (T_i) of 13 min. The reaction conditions were: $T = 47°C$, $[M] = 5.75\ mol\ l^{-1}$ of water, $[E] = 0.103\ mol\ l^{-1}$ of oil, $[AIBN] = 4.02\ mmol\ l^{-1}$ of oil, $\Phi_{w/o} = 1:1$, $N = 1000$ rpm

dilatometry, where an 8.6% decrease in volume was observed for polymerizations with equiphase ratio of oil to water. This was monitored by the oil level of a burette placed above the completely filled reactor. These results agreed well with gravimetric and densitometric measurements.

Further details of the polymerization experiments have been reported elsewhere[32].

The molecular weights were determined by viscometric measurements in 0.1 M aqueous Na_2SO_4 solutions using the Mark–Houwink parameters of Klein[33].

The number of particles and the particle-size distribution were determined by scanning electron microscopy, and dynamic light scattering.

Details of the monomer partitioning experiments between Isopar and water have been reported elsewhere[34]. For acrylamide with 6 wt% sorbitan monooleate and a phase ratio of oil to water of 1:1, the ratio of organic to aqueous monomer is 0.015:1. This agrees quite well with acrylamide partitioning measurements between toluene and water (0.02:1)[35].

High-temperature light scattering studies were performed on a Chromatix KMX-6 LALLS photometer with a cell length of 15 mm and a field stop of 0.2. This corresponded to an average scattering angle of 4.8°. A 0.45 μm cellulose-acetate–nitrate filter (Millipore) was used for polymer solutions. A 0.22 μm filter of the same type was used to clarify the solvent. Distilled deionized water with 0.02 M Na_2SO_4 (analytical grade) was used as a solvent. Temperature control was excellent and was always within 0.1°C.

RESULTS AND DISCUSSION

Experiments have indicated that the rate of polymerization can be expressed as follows:

$$R_p \propto [I]^{1.0}[M]^{1.0}/[E]^a$$

where a is a constant equal to 0.2 for acrylamide polymerizations.

The first-order monomer dependence is normal in free-radical polymerizations and has been reported for heterophase acrylamide polymerizations previously[23,24]. However, the inverse dependence on emulsifier concentration is contrary to what would be expected if the emulsifier's sole function was stabilization. In such cases, increasing the level of emulsifier would lower the surface tension and produce a larger number of smaller particles. Since the total interfacial area would be larger, the capture efficiency of primary radicals would rise and the rate would increase. Since we and others[35] have observed inverse relationships between bulk emulsifier level and rate, there must be additional effects to consider. It is believed that sorbitan monooleate, which saturates the interface at relatively low levels, with the remainder residing in the continuous phase, reacts with primary radicals through the double bond in the oleic acid backbone. Therefore, the addition of higher levels of SMO increases the radical scavenging efficiency and reduces the rate. To test this hypothesis, a series of experiments were performed with a sorbitan monostearate, a chemically identical emulsifier with no unsaturation. All conditions of the experiments were the same as those with SMO: temperature 47°C, acrylamide concentration $5.75\ mol\ l^{-1}$ of oil, emulsifier concentration $0.103\ mol\ l^{-1}$ of oil, rate of agitation 1000 rpm, AIBN concentration $4.02\ mmol\ l^{-1}$ of oil, phase ratio of oil to water 1:1. In polymerizations with SMS the rate was significantly faster, confirming that the presence of double bonds in the emulsifier influences the kinetics by consuming primary radicals in the oil phase.

The observed order of the rate with respect to the initiator level is also peculiar. *Figure 2* shows the rate plotted against [I] and $[I]^{1/2}$. Clearly the traditional one-half order dependence is not observed. This indicates the presence of a unimolecular termination reaction which competes with the bimolecular step and is more favourable at lower macroradical levels. In general, unimolecular termination involves the reaction of a polymeric radical with a small molecule, such as solvent, initiator or emulsifier. Since the solvent used for inverse-microsuspension is water and AIBN has not been observed to have any significant transfer activity, the emulsifier seems the most probable candidate. This has been confirmed by previous investigations of inverse-microsuspensions with water-soluble initiators[26,30],

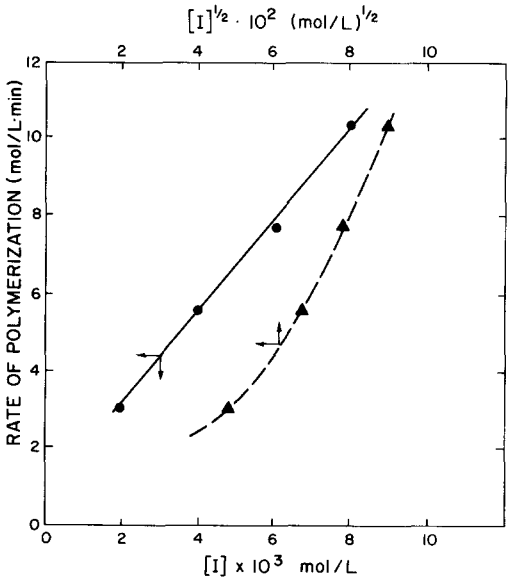

Figure 2 Rate of polymerization (R_p) *versus* the first (●) and half (▲) powers of initiator (AIBN) concentration. Experimental conditions were: $T = 47°C$, $[M] = 5.75\ mol\ l^{-1}$ of water, $[E] = 0.103\ mol\ l^{-1}$ of oil, $\Phi_{w/o} = 1:1$, $N = 1000$ rpm

Table 3 Weight-average molecular weights of polyacrylamides produced in solution[a] with and without sorbitan monooleate

Without sorbitan monooleate, $\bar{M}_w$ (g mol^{-1}) $\times 10^{-6}$	With sorbitan monooleate[b] $\bar{M}_w$ (g mol^{-1}) $\times 10^{-6}$
3.0	3.3
2.7	3.5
2.6	3.3
2.9	
Average 2.80	3.37

[a] Reaction conditions were: temperature, 50°C; acrylamide concentration, 1.41 mol l^{-1}; initiator ($K_2S_2O_8$) concentration, 1×10^{-3} mol l^{-1}

[b] Emulsifier concentration 0.091 mol l^{-1}

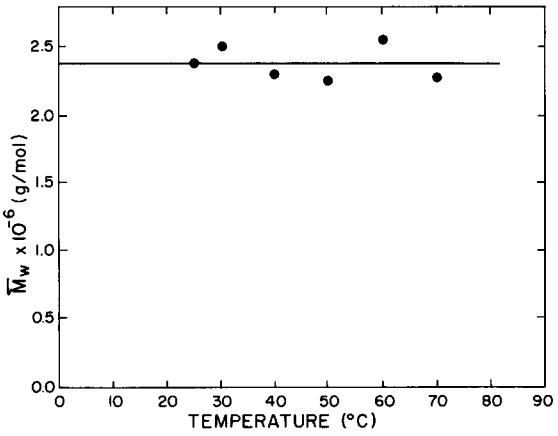

Figure 3 Weight-average molecular weight ($\bar{M}_w$) as a function of measurement temperature. The polymer was prepared in aqueous solution in the presence of sorbitan monooleate. The experimental conditions are listed in *Table 3*

where transfer to the stearic and oleic acid portions of the emulsifier has been found to be rate-controlling, and for inverse-emulsion polymerization with oil-soluble initiators[24].

To confirm the transfer activity of sorbitan monooleate a series of solution polymerizations were performed both with and without emulsifier. The conditions and final weight-average molecular weights are reported in *Table 3*. On average, polymerizations with emulsifier gave molecular weights 19% larger. This increase is presumed to be due to one of two factors:

(1) The reaction of macroradicals with emulsifier followed by agglomeration of the hydrophobic ends of the polymer molecules to yield an apparent molecular weight that was higher than actual.

(2) Extraction of a hydrogen from the hydrophilic portion of the emulsifier to form a dead polymer molecule and an emulsifier radical. When this polymerizes it would generate a macroradical with a terminal double bond which could later react to form a branched polymer*.

To distinguish between branching and agglomeration, high-temperature light scattering has been recommended[36]. This has been found to be an ideal method of identifying agglomeration since as the temperature rises the additional energy is able to break loose flocks but is insufficient to cleave bonds. *Figure 3* shows no trend in the measured weight-average molecular weight between 25 and 80°C. Therefore, the rise in molecular weight observed in solution polymerizations with sorbitan monooleate is more likely due to branching. The proposed mechanism for this is shown in *Figure 4*. This mechanism has been further verified by comparing inverse-microsuspension polymerizations with sorbitan monooleate and sorbitan monostearate under the same conditions. SMS polymerizations gave molecular weights 30% lower (3.5×10^6 vs. 5×10^6), primarily due to the absence of unsaturation which eliminates long-chain branching.

Experiments have also indicated that the rate of polymerization is dependent on the level of agitation. This must be due to a mass transfer limitation of one of the reacting species. Since primary radicals are the only species to have appreciable concentrations in both phases, their diffusion is believed to be rate-controlling. Higher rates of agitation generate smaller particles and larger interfacial areas which improve mass transfer and increase the polymerization rate.

Based on these observations a general mechanism for homopolymerizations will be presented in the next section. This will be evaluated against experimental conversion, molecular-weight and particle-size data for acrylamide polymerizations. Once verified, we will be able to use the resulting kinetic model to improve polymerization procedures. This includes isolating the conditions under which the highest-molecular-weight polymer is obtained.

MECHANISM

Reactions in the oil phase

1. $I \xrightarrow{k_d} 2R^{\bullet}_{in,o}$
2. $R^{\bullet}_{in,o} + E_o \xrightarrow{k_1}$ inert products
3. $R^{\bullet}_{in,o} + HC \xrightarrow{k_4}$ inert products
4. $R^{\bullet}_{in,o} + M_o \xrightarrow{k_p} R^{\bullet}_{1,o}$
5. $R^{\bullet}_{r,o} + M_o \xrightarrow{k_p} R^{\bullet}_{r+1,o}$

where $R^{\bullet}_{in,o}$, HC, E_o, M_o and $R^{\bullet}_{r,o}$ are the symbols for

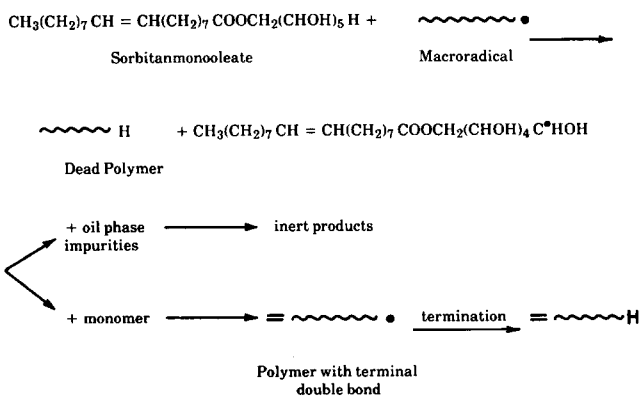

Figure 4 The proposed reaction mechanism of interfacial emulsifier (SMO) with macroradicals

* Transfer to monomer also generates terminal double bonds which have been found to be unreactive, since branching has not been detected in solution polymerizations of acrylamide[1-11,41-43]

primary radicals, hydrocarbon, emulsifier, monomer and macroradicals in the oil phase.

Transfer between phases

6. $R^{\bullet}_{in,o} \xrightarrow{k_r} R^{\bullet}_{in,w}$
7. $R^{\bullet}_{r,o} \xrightarrow{k_{r,r}} R^{\bullet}_{r,w}$
8. $M_o \overset{\Phi_m}{\rightleftarrows} M_w$

where the subscript w denotes a water-phase concentration, and $k_{r,r}$ is the mass transfer constant of an oligoradical of length r, which will tend to k_r at small chain lengths.

Water-phase reactions

9. $R^{\bullet}_{in,w} + M_w \xrightarrow{k_p} R^{\bullet}_{1,w}$
10. $R^{\bullet}_{r,w} + M_w \xrightarrow{k_p} R^{\bullet}_{r+1,w}$
11. $''R^{\bullet}_{r,w} + M_w \xrightarrow{k_p} ''R^{\bullet}_{r+1,w}$
12. $R^{\bullet}_{r,w} + \Gamma_E \xrightarrow{k_{fe}} P_r + E^{\bullet}$
13. $''R^{\bullet}_{r,w} + \Gamma_E \xrightarrow{k_{fe}} ''P_r + E^{\bullet}$
14. $E^{\bullet} + M_w \xrightarrow{k_p} ''R^{\bullet}_{1,w}$
15. $E^{\bullet} + HC_{imp} \xrightarrow{k_s}$ inert products
16. $R^{\bullet}_{r,w} + M_w \xrightarrow{k_{fm}} P_r + R^{\bullet}_{1,w}$
17. $''R^{\bullet}_{r,w} + M_w \xrightarrow{k_{fm}} ''P_r + R^{\bullet}_{1,w}$
18. $R^{\bullet}_{r,w} + R^{\bullet}_{s,w} \xrightarrow{k_{td}} P_r + P_s$
19. $''R^{\bullet}_{r,w} + R^{\bullet}_{s,w} \xrightarrow{k_{td}} ''P_r + P_s$
20. $''R^{\bullet}_{r,w} + ''R^{\bullet}_{s,w} \xrightarrow{k_{td}} ''P_r + ''P_s$
21. $''P_{r,w} + R^{\bullet}_{s,w} \xrightarrow{k^*} R^{\bullet}_{r+s,w}$
22. $''P_{r,w} + ''R^{\bullet}_{s,w} \xrightarrow{k^*} ''R^{\bullet}_{r+s,w}$

where $''R^{\bullet}$ is a radical that contains a terminal emulsifier double bond, Γ_E is the surface concentration of emulsifier, $E^{\bullet}$ is the symbol for emulsifier radicals and HC_{imp} represents hydrocarbon-phase impurities or radicals.

The mechanism can be generally described as a free-radical heterophase polymerization in which mass transfer of primary radicals and oligoradicals between the organic and aqueous phases is important. Termination occurs by both unimolecular (steps 12 and 13) and bimolecular (steps 18 to 20) reactions, the latter being exclusively disproportionation. Unimolecular termination produces emulsifier radicals that contain double bonds. These radicals can either propagate with monomer (step 14) or terminate with oil-phase impurities (step 15). When propagation occurs, macroradicals are produced which can react to form a branched polymer (steps 21 and 22). The remaining steps in the mechanism are initiation, propagation, transfer and termination reactions, which are common to any free-radical mechanism. Initiation is assumed to occur by primary radicals in the oil phase reacting with slightly soluble acrylamide to form oligoradicals which quickly reach their solubility limit and diffuse into the oil phase. Primary radicals may also diffuse into the monomer droplets unreacted and propagate.

KINETIC MODEL

Initiation

Applying the stationary-state hypothesis to primary radicals in the oil and water phases we obtain:

$$d[R^{\bullet}_{in,o}]/dt \simeq 0 = 2k_d[I] - k_p[R^{\bullet}_{in,o}][M_o] - k_4[R^{\bullet}_{in,o}][HC] - k_1[R^{\bullet}_{in,o}][E_o] - (k_r/V_o)([R^{\bullet}_{in,o}]/\Phi_r - [R^{\bullet}_{in,w}]) \quad (1)$$

and

$$d[R^{\bullet}_{in,w}]/dt \simeq 0 = (k_r/V_w)([R^{\bullet}_{in,o}]/\Phi_r - [R^{\bullet}_{in,w}]) - k_p[R^{\bullet}_{in,w}][M_w] \quad (2)$$

where V_o and V_w are the volume of the oil and water phases and Φ_r is the partition coefficient of primary radicals between oil and water.

From partitioning measurements, we can express the concentration of monomer in the oil phase as:

$$[M_o] = \Phi_m[M_w]$$

Adding (1) and (V_w/V_o) times (2) and rearranging, one obtains:

$$[R^{\bullet}_{in,o}] = \frac{2k_d[I] - k_p[M_w][R^{\bullet}_{in,w}](V_w/V_o)}{k_p\Phi_m[M_w] + k_4[HC] + k_1[E_o]} \quad (3)$$

Substituting (3) into (2) and solving for $[R^{\bullet}_{in,w}]$ yields:

$$[R^{\bullet}_{in,w}] = 2k_d[I]\gamma/\delta \quad (4)$$

where

$$\gamma = \frac{k_r}{V_w\Phi_r}\left(\frac{1}{k_p[M_w] + k_r/V_w}\right)\left(\frac{1}{k_p\Phi_m[M_w] + k_4[HC] + k_1[E_o]}\right) \quad (5)$$

and

$$\delta = 1 + \frac{k_r}{V_w\Phi_r}\left(\frac{1}{k_p[M_w] + k_r/V_w}\right)\left(\frac{k_p[M_w]V_w/V_o}{k_p\Phi_m[M_w] + k_4[HC] + k_1[E_o]}\right) \quad (6)$$

Now, if we assume that the main source of initiation is the diffusion of primary radicals into polymer particles, we can define the rate of initiation as:

$$R_i = k_p[M_w][R^{\bullet}_{in,w}] = 2k_d[I]\left(\frac{k_p[M_w]\gamma}{\delta}\right) \quad (7)$$

We may also say that

$$R_i = 2fk_d[I] \quad (8)$$

Comparing these two definitions of the rate of initiation, we have an expression for f, the efficiency of initiation:

$$f = k_p[M_w]\gamma/\delta$$

which can be 'simplified' to yield:

$$f = \left[1 + \frac{V_o\Phi_r}{k_r}\left(1 + \frac{k_r}{k_p[M_w]V_w}\right)(k_p\Phi_m[M]_w + k_4[HC] + k_1[E_o])\right]^{-1}\frac{V_o}{V_w}$$

$k_p[M]$ is large, and k_r is of the order 10^{0-3}; therefore:

$$1+k_r/k_p[M_w]V_w \simeq 1$$

Defining the overall mass transfer constant (k_r) as:

$$k_r = k_r^* A_T$$

and

$$A_T = a_{sp} V_o$$

where A_T is the total interfacial area and a_{sp} is the specific interfacial area per litre of oil.

Now f can be reduced to:

$$f = \left[1+\frac{\Phi_r}{k_r^*}\left(\frac{k_p\Phi_m[M_w]}{a_{sp}}+\frac{k_4[HC]}{a_{sp}}+\frac{k_1[E_o]}{a_{sp}}\right)\right]^{-1}\frac{V_o}{V_w} \quad (9)$$

This can be further simplified for conditions where f is not observed to be a function of conversion to yield:

$$f = \left[1+\frac{\Phi_r}{k_r^*}\left(\frac{k_4[HC]}{a_{sp}}+\frac{k_1[E_o]}{a_{sp}}\right)\right]^{-1}\frac{V_o}{V_w} \quad (10)$$

Rate of polymerization

We can now apply the stationary-state hypothesis to macroradicals with no unsaturated carbons [R•], to macroradicals that contain a terminal emulsifier double bond [″R•], and to emulsifier radicals [E•]:

$$d[R^\bullet]/dt \simeq 0 = R_I - k_{td}[R^\bullet]([R^\bullet]+[''R^\bullet]) - k_{fe}[R^\bullet]\Gamma_E + k_{fm}[M_w][''R^\bullet] \quad (11)$$

$$d[''R^\bullet]/dt \simeq 0 = k_p[E^\bullet][M_w] - k_{td}[''R^\bullet]([R^\bullet]+[''R^\bullet]) - k_{fe}[''R^\bullet]\Gamma_E - k_{fm}[M_w][''R^\bullet] \quad (12)$$

$$d[E^\bullet]/dt \simeq 0 = k_{fe}([R^\bullet]+[''R^\bullet])\Gamma_E - k_p[E^\bullet][M_w] - k_5[HC_{imp}][E^\bullet] \quad (13)$$

where

$$[R^\bullet] = \sum_{r=1}^{\infty}[R_r^\bullet]$$

and

$$[''R^\bullet] = \sum_{r=1}^{\infty}[''R_r^\bullet]$$

The total macroradical concentration $[R_T^\bullet]$ is given by:

$$[R_T^\bullet] = [R^\bullet]+[''R^\bullet]$$

Adding equations (11) and (12):

$$R_I - k_p[E^\bullet][M_w] - k_{td}[R_T^\bullet]^2 - k_{fe}[R_T^\bullet]\Gamma_E = 0 \quad (14)$$

where the rate of initiation of emulsifier radicals is:

$$R_{I,e} = k_p[M_w][E^\bullet] \quad (15)$$

Rearranging equation (14) and combining with (15) yields:

$$R_{1,e} = \frac{k_{fe}[R_T^\bullet]\Gamma_E}{1+k_5[HC_{imp}]/k_p[M_w]}$$

The rate of initiation of emulsifier radicals can also be expressed as:

$$R_{I,e} = f_e k_p[R_T^\bullet]\Gamma_E \quad (16)$$

Therefore, we can define the efficiency of initiation of emulsifier radicals (f_e) as:

$$f_e = \frac{1}{1+k_5[HC_{imp}]/k_p[M_w]} \quad (17)$$

Substituting equations (16) and (17) into (14), we obtain a quadratic expression for the total macroradical concentration:

$$2fk_d[I] - k_{td}[R_T^\bullet]^2 - (1-f_e)k_{fe}[R_T^\bullet]\Gamma_E = 0 \quad (18)$$

Now, we apply the long-chain approximation, which assumes that monomer is consumed entirely in propagation in the aqueous phase and that the monomer consumed in the following steps is negligible:

(i) transfer to monomer,
(ii) reaction between emulsifier radical and monomer,
(iii) propagation in the oil phase to form oligoradicals.

Therefore, the rate of polymerization is:

$$R_p = k_p[M_w][R_T^\bullet]$$

We can now examine two extreme cases.

Case 1 (unimolecular termination dominates)

$$k_{fe}[R_T^\bullet]\Gamma_E \gg k_{td}[R_T^\bullet]^2$$

and

$$R_p = \frac{2fk_dk_p[I][M]}{(1-f_e)k_{fe}\Gamma_E}$$

This suggests that the rate of polymerization is proportional to the initiator concentration, which is what we and others have observed for inverse-microsuspension polymerization of acrylamide. We also see that the rate is inversely proportional to the surface emulsifier level. Experimentally, we have observed a dependence that is order 0.2 with respect to the bulk emulsifier. The difference between these two orders is due to the difference between bulk and interfacial concentrations. This will be discussed further in the next section.

Case 2 (bimolecular termination dominates)

$$k_{fe}[R_T^\bullet]\Gamma_E \ll k_{td}[R_T^\bullet]^2$$

and

$$R_p = \left(\frac{2fk_d[I]}{k_{td}}\right)^{1/2}k_p[M]$$

which is the classical free-radical polymerization equation.

In inverse-microsuspension, the contribution of unimolecular termination decreases as the reaction proceeds, and a transition from Case 1 to Case 2 occurs.

At high conversions, termination and the reaction with terminal double bonds will be diffusion-controlled. This has been modelled using the following empirical equations:

$$k_{td} = k_{td}^0/\exp(Aw_p)$$

$$k^* = k^{*0}/\exp(Aw_p)$$

where

$$A = a_0 + a_1 T$$

and T is the temperature in Kelvin and w_p is the weight fraction of polymer in the aqueous phase. The magnitude of the diffusion limitation of these two reactions is assumed to be the same, as a first approximation.

Molecular weights

Using the method of moments the following equations have been derived for the number- and weight-average molecular weights ($\bar{M}_n$ and $\bar{M}_w$):

$$\bar{M}_n = M_m Q_{1T}/Q_{0T}$$

$$\bar{M}_w = M_m Q_{2T}/Q_{1T}$$

where M_m is the molecular weight of the monomer, Q_i is the ith moment of the distribution of polymer molecules without terminal double bonds, $''Q_i$ is the ith moment of the distribution of polymer molecules that contain terminal double bonds, and Q_{iT} is the ith moment of the total dead polymer distribution ($Q_{iT} = Q_i + ''Q_i$). These moments may be solved using the following equations:

$$dQ_0/dt = Y_0 X$$

$$d''Q_0/dt = ''Y_0 X - k^* ''Q_0 Y_{0T}$$

$$dQ_1/dt = Y_1 X$$

$$d''Q_1/dt = ''Y_1 X - k^* ''Q_1 Y_{0T}$$

$$dQ_2/dt = Y_2 X$$

$$d''Q_2/dt = ''Y_2 X - k^* ''Q_2 Y_{0T}$$

where

$$X = k_{fe}\Gamma_E + k_{fm}M + k_{td}Y_{0T}$$

$''Y_i$, Y_i are the moments of the macroradical distribution for molecules with and without terminal double bonds, respectively, and Y_{iT} is the ith moment of the total macroradical distribution ($Y_{iT} = Y_i + ''Y_i$).

The zeroth, first and second moments of the macroradical distribution are given by:

$$Y_0: \quad 0 = R_I - k_{fe}\Gamma_E Y_0 + k_{fm}M\,''Y_0 - k_{td}Y_0(Y_{0T})$$

$$''Y_0: \quad 0 = R_I' - k_{fe}\Gamma_E\,''Y_0 - k_{fm}M\,''Y_0 - k_{td}\,''Y_0(Y_{0T})$$

$$Y_{0T}: \quad 0 = R_I + R_I' - k_{fe}\Gamma_E Y_{0T} - k_{td}(Y_{0T})^2$$

$$Y_1 = \frac{R_I + k_{fm}MY_{0T} + k_pMY_0 + k^*Y_0\,''Q_1}{X}$$

$$''Y_1 = \frac{R_I' + k_pM\,''Y_0 + k^*\,''Y_0\,''Q_1}{X}$$

$$Y_{1T} = \frac{R_I + R_I' + k_pMY_{0T} + k^*Y_{0T}\,''Q_1 + k_{fm}MY_{0T}}{X}$$

$$Y_2 = \frac{R_I + 2k_pMY_1 + k_{fm}MY_{0T} + k^*(Y_0\,''Q_2 + 2Y_1\,''Q_1)}{X}$$

$$''Y_2 = \frac{R_I' + 2k_pM\,''Y_1 + k^*(''Y_0''Q_2 + 2\,''Y_1\,''Q_1)}{X}$$

$$Y_{2T} = \frac{R_I + R_I' + 2k_pMY_{1T} + k_{fm}MY_{0T} + k^*(Y_{0T}''Q_2 + 2Y_{1T}''Q_1)}{X}$$

Emulsifier concentration in the boundary layer

The distribution of emulsifier between the continuous phase and the surface of the particles* has been modelled with a Langmuir adsorption isotherm. The fractional coverage of the surface of the polymer particles (θ) is given by:

$$\theta = \frac{v}{v_m} = \frac{K[E_o]}{1 + K[E_o]} \tag{19}$$

where v is the volume of emulsifier adsorbed and v_m is the maximum volume adsorbed if the monolayer is completely full. K is the equilibrium adsorption constant†.

The surface concentration of emulsifier can be expressed as:

$$\Gamma_{E,bl} = \frac{v\rho_E}{MW_E A_T} \tag{20}$$

where ρ_E and MW_E are the density and molecular weight of the emulsifier and A_T is the total interfacial area.

The moles of emulsifier in the oil phase ($N_{E,o}$) can be calculated from the difference between total (N_E) and interfacial emulsifier ($N_{E,bl} = \Gamma_{E,bl}A_T$):

$$N_{E,o} = N_E(v\rho_E/MW_E)$$

From this, the emulsifier concentration in the organic phase is given by:

$$[E_o] = \frac{N_E MW_E - v\rho_E}{V_o MW_E} \tag{21}$$

To solve equations (19) to (21) requires an expression for the volume of a complete monolayer (v_m). This can be obtained through a balance on the total area occupied by the emulsifier (A_E). A_E can be defined as the fraction of the total area occupied (θA_T) and equivalently by the number of emulsifier molecules at the interface, multiplied by the

* The solubility of emulsifier in the aqueous phase is essentially zero

† In order to obtain steric stabilization in inverse microsuspensions, the surface must be rigid and almost completely covered. Therefore, the equilibrium constant will be quite large

area occupied by each molecule (A_p):

$$A_E = \theta A_T = \left(\frac{v\rho_E N_A}{MW_E}\right) A_p$$

Rearranging this expression in terms of v_m yields:

$$v_m = \frac{MW_E A_T}{\rho_E N_A A_p} \tag{22}$$

where the area occupied by a single molecule of sorbitan monooleate has been determined to be 69 Å^2 using a Wilhelmy balance.

Equations (19) to (21) represent a set of equations that can be used to calculate the surface and continuous-phase concentrations of emulsifier, as well as the fractional coverage of the polymer particles.

Particle size

Predicting the drop size in mechanically agitated systems requires understanding the break-up and coalescence mechanisms. Drop break-up occurs when the kinetic energy of droplet oscillations, caused by turbulence, exceeds the surface energy of the droplet. By balancing these two factors Sprow[37] has shown that the volume-to-surface average diameter (d_{32}) can be expressed as:

$$d_{32}/D = CW_e^{-3/5} \tag{23}$$

where D is the impeller diameter and C is a constant. The Weber number is defined as:

$$W_e = \rho N^2 D^3/\sigma$$

where N is the rate of agitation (rps), ρ is the density of the continuous phase* and σ is the surface tension.

The turbulence will also cause droplets to collide with each other. If these droplets remain in contact long enough for the intervening film of liquid to drain, coalescence will occur. In heterogeneous polymerizations, this is prevented through the addition of electrostatic or steric stabilizers.

In polymeric reactions, where dispersed-phase volume fractions of 50% or more are common, the effect of hold-up must also be considered. Larger hold-ups, which dampen the turbulence intensity, will result in larger drop sizes. This is usually expressed by the empirical equation:

$$d_{32} = d_{32}^0(1 + C_2\Phi) \tag{24}$$

where d_{32}^0 is the volume-to-surface diameter at low hold-ups ($\Phi = V_w/(V_w + V_o)$). Combining equations (23) and (24) yields:

$$d_{32}/D = C_1(1 + C_2\Phi)W_e^{-3/5} \tag{25}$$

Several combinations of C_1 and C_2 exist in the literature[39–44]. For suspension polymerization, the Lee and Tasakorn[43] equation has been recommended, where $C_1 = 0.063$ and $C_2 = 1.81$. This was developed for high hold-ups, in a sterically stabilized system which is very similar to inverse microsuspensions, and is used in this paper.

*For Isopar-M, the density (g cm^{-3}) is given by $\rho = 0.995 - 7.047 \times 10^{-4}T$, where the temperature is in kelvins

From our experiments, we have correlated the surface tension with the emulsifier concentration, rate of agitation and temperature as:

$$\sigma = a[E]^{-0.293}N^{1.44}$$

where $a = 5.67 \times 10^{-6} - 1.71 \times 10^{-8}T$. This equation will be restricted to systems with the same reactor configuration as was used in this work. For other systems, similar correlations can be established. In the absence of surface tension measurements, the experimental value of d_{32} can be used directly in the rate expression.

The number of particles (N_p) can be computed from the volume average diameter (d_v) as follows:

$$N_p = \frac{\text{volume of the dispersed phase}}{\text{volume of one particle}} = \frac{V_w}{(\pi/6)d_v^3}$$

where the volume average diameter is related to the surface-to-volume diameter as[44]:

$$d_v = \frac{\alpha_s}{(6\alpha_v)^{2/3}\pi^{1/3}} d_{32}$$

For a monodisperse system of spherical particles, the proportionality constant between d_v and d_{32} is 1.0. In the system studied in this work, the proportionality constant was found to be 1.363, the larger value being due to the breadth of the particle size distribution.

SUMMARY OF KINETIC MODEL

Table 4 summarizes the equations needed to model rate, molecular weight, particle size and particle number for inverse-microsuspension homopolymerizations. These can be solved analytically with the exception of the differential equations for monomer consumption and the moments of the molecular-weight distribution, which must be solved numerically. In the simulations done for this paper a variable-order Runge–Kutta procedure was used.

PARAMETER ESTIMATION

When the model is applied to the polymerization of a specific monomer, several rate, mass transfer and partition coefficients are needed. In the absence of available literature values these must be estimated from experimental data. In this work parameters were determined by non-linear weighted least-squares regression using Marquardt's procedure to minimize the sum of squares of the residuals. The total residual comprised two independent measurements, conversion and weight-average molecular weight, which were weighted by the reciprocal of their variances as follows:

$$\text{Min} \sum_{i=1}^{n} \left[\left| \left(\frac{X_{i,p} - X_{i,d}}{\sigma_{X,i}^2} \right) \right| + \left| \left(\frac{MW_{i,p} - MW_{i,d}}{\sigma_{MW,i}^2} \right) \right| \right]^2$$

where n is the number of observations, $X_{i,p}$ and $X_{i,d}$ are the predicted and measured conversions, $MW_{i,p}$ and $MW_{i,d}$ are the model and experimental weight-average molecular weights, and $\sigma_{X,i}^2$ and $\sigma_{MW,i}^2$ are the variances of the ith conversion and molecular-weight measurements.

Table 5 lists the parameters used for simulations of acrylamide homopolymerizations. The important conclusions from the parameter estimation are summarized below:

(1) The transfer to monomer constant is roughly twice as large as has been reported for solution polymerizations[6,47,48]. The difference is probably due to the presence of interfacial acrylamide in inverse microsuspension[49]. This monomer would reside with the amide group in the aqueous phase and the vinyl group oriented towards or in the emulsifier boundary layer. In such a configuration the labile hydrogens will be more accessible than the double bond, which will increase the likelihood of transfer relative to propagation.

(2) The transfer to emulsifier and surface emulsifier equilibrium constant were determined individually at 47°C. However, the temperature dependences could not be estimated independently and therefore transfer to emulsifier and the interfacial emulsifier concentration were fitted as a single parameter. The activation energy is positive, which is typical in physical adsorption and also indicates that the contribution of transfer to emulsifier to the grouped activation energy is small. This is consistent with other termination reactions, which have very low temperature dependences. To determine the individual values of k_{fe} and Γ_E requires knowledge of the emulsifier partitioning between the continuous phase and the interface at different temperatures.

(3) The individual values of the parameters k_1, k_4, Φ_r and k_r^* cannot be determined without further experimentation into the partitioning and mass transfer of primary radicals between the oil and water phases. For the purpose of modelling the parameters were fitted as two grouped rate constants:

$$\left(\frac{k_1\Phi_r}{k_r^*}\right) \quad \text{and} \quad \left(\frac{k_4\Phi_r}{k_r^*}\right)$$

as they appear in the expression for rate of polymerization.

(4) The rate constant for propagation with terminal emulsifier double bonds was determined to be roughly twice the propagation rate constant. This is reasonable since both reactions involve a macroradical and an unsaturated carbon, and should be similar in magnitude.

Table 4 Summary of kinetic model equations

Rate	
Rate of polymerization	$R_p = k_p[M]_w[R_T^\cdot]$
Total macroradical concentration	$0 = 2fk_d[I] - k_{td}[R_T^\cdot]^2 - (1-f_e)k_{fe}[R_T^\cdot]$
Efficiency of initiation of primary radicals	$f = \left[1 + \left(\frac{k_1\Phi_r}{k_r^*}\right)\frac{[E]_o}{a_{sp}} + \left(\frac{k_4\Phi_r}{k_r^*}\right)\frac{[HC]}{a_{sp}}\right]^{-1}\frac{V_o}{V_w}$
Efficiency of initiation of emulsifier radicals	$f_e = \frac{1}{1 + k_5[HC_{imp}]/k_p[M]_w}$
Molecular weights	
Number-average molecular weight	$\bar{M}_n = M_m Q_{1T}/Q_{0T}$
Weight-average molecular weight	$\bar{M}_w = M_m Q_{2T}/Q_{1T}$
	where Q_{0T}, Q_{1T} and Q_{2T} are the zeroth, first and second moments of the dead polymer distribution
Emulsifier distribution	
Surface emulsifier concentration	$\Gamma_{E,bl} = \frac{v\rho_E}{MW_E A_T}$
Continuous-phase emulsifier concentration	$[E]_o = \frac{N_E MW_E - v\rho_E}{V_o MW_E}$
Fractional coverage of interface	$\theta = \frac{v}{v_m} = \frac{K[E]_o}{1 + K[E]_o}$
Volume of a complete monolayer	$v_m = \frac{MW_E A_T}{\rho_E N_A A_p}$
Particle characteristics	
Average surface–volume diameter	$d_{32}/D = 0.063(1 + 1.81\Phi)W_c^{-0.6}$
Number of particles	$N_p = \frac{V_w}{(\pi/6)d_v^3}$
Volume average diameter	$d_v = \frac{\alpha_s}{(6\alpha_v)^{2/3}\pi^{1/3}}d_{32}$

EVALUATING THE KINETIC MODEL AGAINST EXPERIMENTAL DATA

The kinetic model is compared with experimental conversion, molecular-weight, particle-size and number

Table 5 Summary of parameter values

Parameter	Value	Units	Source
$k_{d,AIBN}$	$9.48 \times 10^{16}\exp(-30\,800/RT)$	min^{-1}	45
$k_{d,ADVN}$	$4.316 \times 10^{16}\exp(-29\,000/RT)$	min^{-1}	46
k_p	$9.9 \times 10^7\exp(-2743/RT)$	$l\,mol^{-1}\,min^{-1}$	3, 47, 48
$k_{td}^{1/2}$	$9.192 \times 10^4\exp(-741/RT)$	$l\,mol^{-1}\,min^{-1}$	3, 47, 48
k_{fm}	$5.73 \times 10^8\exp(-10\,438/RT)$	$l\,mol^{-1}\,min^{-1}$	This work
$k_5[HC_{imp}]$	$0.147\exp(1380.5/T)$	min^{-1}	This work
A	$16.08 - 2 \times 10^{-2}T$	dimensionless	This work
$(k_{fe}\Gamma_E)_{SMO}$[a]	$1.51 \times 10^{-7}\exp(1415/T)/d_{32}$	min^{-1}	This work
$(k_{fe}\Gamma_E)_{SMS}$[b]	$1.05 \times 10^{-7}\exp(1415/T)/d_{32}$	min^{-1}	This work
k_{SMO}^*	$1.74k_p$	$l\,mol^{-1}\,min^{-1}$	This work
k_{SMS}^*	0.0	$l\,mol^{-1}\,min^{-1}$	This work
$(k_1\Phi_r/k_r^*)_{AIBN}$	1.05×10^3	$m^2\,mol^{-1}$	This work
$(k_1\Phi_r/k_r^*)_{ADVN}$	1.22×10^3	$m^2\,mol^{-1}$	This work
$(k_4\Phi_r/k_r^*)_{AIBN,SMO}$	4.14×10^4	$m^2\,mol^{-1}$	This work
$(k_4\Phi_r/k_r^*)_{ADVN,SMO}$	4.81×10^4	$m^2\,mol^{-1}$	This work
$(k_4\Phi_r/k_r^*)_{SMS}$	0.0	$m^2\,mol^{-1}$	This work

[a] At 47°C, $\Gamma_E = 2.40 \times 10^{-6}\,mol\,m^{-2}$ and $k_{fe} = 5.20/d_{32}$
[b] At 47°C, $\Gamma_E = 2.40 \times 10^{-1}\,mol\,m^{-2}$ and $k_{fe} = 3.64/d_{32}$

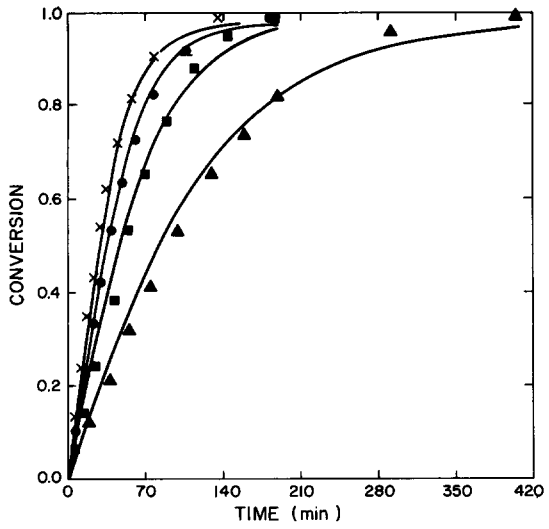

Figure 5 Conversion–time data and model predictions (———) for polymerizations with AIBN initiators at the following conditions: $T=47°C$, $[M]=5.75\,mol\,l^{-1}$ of water, $[E]=0.103\,mol\,l^{-1}$ of oil, $\Phi_{w/o}=1:1$, $N=1000$ rpm; $[AIBN]=1.92$ (▲), 4.02 (■), 6.03 (●) and 7.92 (×) $mmol\,l^{-1}$ of oil

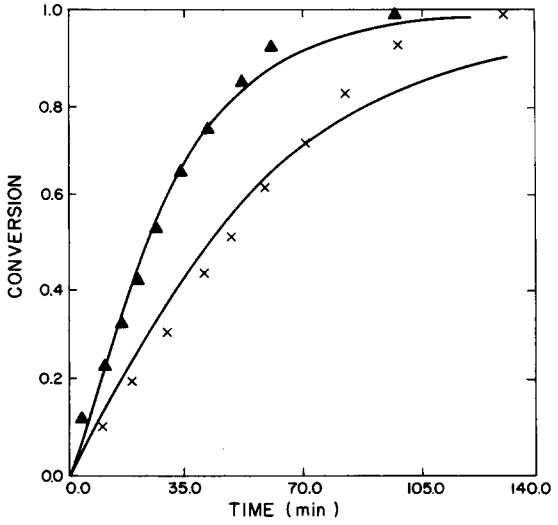

Figure 6 Conversion–time data and model predictions (———) for ADVN initiators. The reaction conditions were: $T=47°C$, $[M]=5.75\,mol\,l^{-1}$ of water, $[E]=0.103\,mol\,l^{-1}$ of oil, $\Phi_{w/o}=1:1$, $N=1000$ rpm; $[ADVN]=0.65$ (×) and 1.33 (▲) $mmol\,l^{-1}$ of oil

data for various levels of initiator, monomer, emulsifier, temperature, rate of agitation and types of initiator and emulsifier. In all cases the model is represented by a full curve and the data by symbols.

The kinetic model can predict the conversion–time behaviour very well over a broad range of initiator levels for two initiators (AIBN, *Figure 5*; ADVN, *Figure 6*). The model also gives good estimates of the terminal weight-average molecular weight at different AIBN concentrations (*Figure 7*) and the trend in molecular weight with conversion (*Figure 8*). The increase in molecular weight at low conversions is caused by unimolecular termination with emulsifier, which produces dead polymer and an emulsifier radical. This radical propagates, to produce polymer which contains a terminal double bond, and later reacts to form a long-chain branch. The molecular weight levels off at high conversions due to the reduced reactivity of the terminal double bonds with macroradicals, which corresponds to a decrease in the formation rate of branched polymers.

The calculated rates of initiation from primary and emulsifier radicals are shown in *Figure 9*. The initiation by emulsifier radicals contributes significantly to the overall rate at the outset of the polymerization and then decreases to zero. This decline is caused by competition for the emulsifier radicals between monomer and organic-phase impurities and radicals. As the reaction proceeds, the emulsifier radical is in an environment with a lower monomer level and has a greater probability of diffusing into the oil phase and terminating.

Figure 10 shows the trend in number- and weight-average molecular weight for two chemically similar emulsifiers, sorbitan monooleate and sorbitan monostearate, distinguished only by the absence of unsaturation in the stearic chain of SMS. When SMS is used, molecular weights are fairly constant with conversion, confirming the linearity of the resulting polymer.

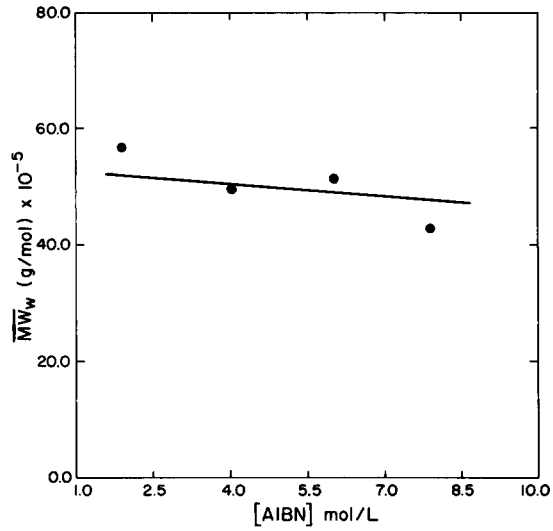

Figure 7 Final weight-average molecular weight ($\overline{MW}_w$) data and model predictions (———) for AIBN polymerizations. Other reaction conditions were the same as in *Figure 5*

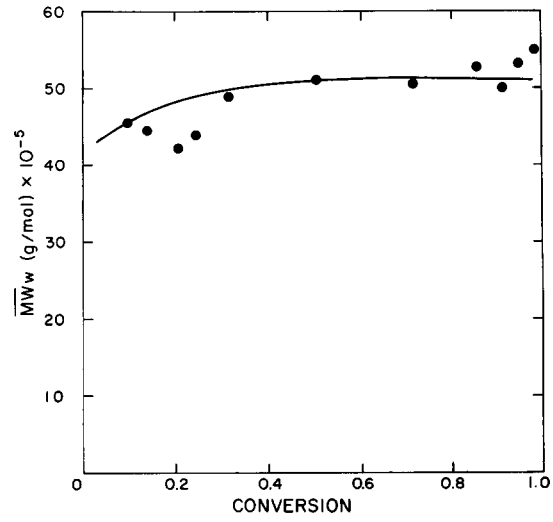

Figure 8 Experimental weight-average molecular weight ($\overline{MW}_w$) data and model predictions (———) for a reaction under the following conditions: $T=47°C$, $[M]=5.75\,mol\,l^{-1}$ of water, $[E]=0.103\,mol\,l^{-1}$ of oil, $[AIBN]=4.02\,mmol\,l^{-1}$ of oil, $\Phi_{w/o}=1:1$, $N=1000$ rpm

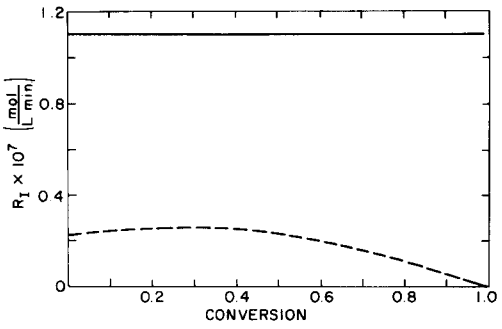

Figure 9 Rate of initiation (R_I) of primary (———) and emulsifier (– – –) radicals as a function of conversion. Conditions of the simulation were the same as in *Figure 8*

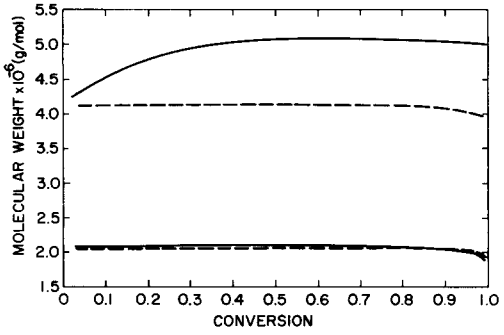

Figure 10 Number- and weight-average molecular weights for polymerizations with sorbitan monooleate (———) and sorbitan monostearate (– – –). Conditions of the simulations were the same as in *Figure 8*

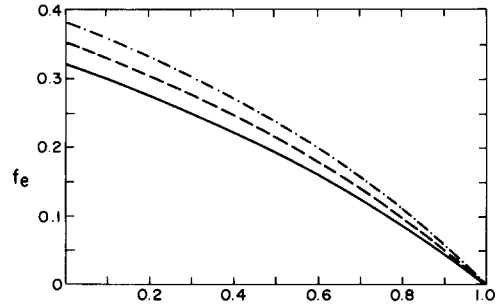

Figure 11 Efficiency of initiation of emulsifier radicals (f_e) as a function of conversion at several temperatures: 40°C (———), 50°C (– – –) and 60°C (– · – · –). The remaining experimental conditions of the simulations were: $[M] = 5.75\ mol\ l^{-1}$ of water, $[E] = 0.103\ mol\ l^{-1}$ of oil, $[AIBN] = 4.02\ mmol\ l^{-1}$ of oil, $\Phi_{w/o} = 1:1$, $N = 1000$ rpm

Increasing the initiator concentration causes a higher fraction of macroradicals to be terminated by a bimolecular process and reduces the fraction of polymer molecules with terminal double bonds. The terminal double bond density is also reduced at higher temperatures, which favour propagation over termination of emulsifier radicals with oil-phase impurities. This increases the efficiency of initiation of emulsifier radicals (*Figure 11*).

Particle size and number were found to be invariant to initiator concentration.

Thermal effects

The model gives good predictions of the conversion of monomer to polymer (*Figure 12*) and final weight-average molecular weight (*Figure 13*) at temperatures between 42 and 57°C. Kinetically, the thermal effects are dominated by two factors: the large activation energy of the decomposition of initiator and the surface tension. At high temperatures the surface tension is reduced, which generates smaller particles in a larger number (*Figures 14* and *15*). Smaller particles generate a larger total interfacial area, which increases the capture of primary radicals and oligoradicals generated in the oil phase and increases the efficiency of initiation (*Figure 16*). The smaller particles also have a higher surface-to-volume ratio, which improves the accessibility of macroradicals to the interfacial emulsifier and increases the transfer to emulsifier.

Figure 17 shows the average number of radicals per particle ($\bar{n}$) as a function of conversion at several temperatures. For typical temperatures of 40 to 50°C, $\bar{n}$ is quite large. At higher temperatures the average number of

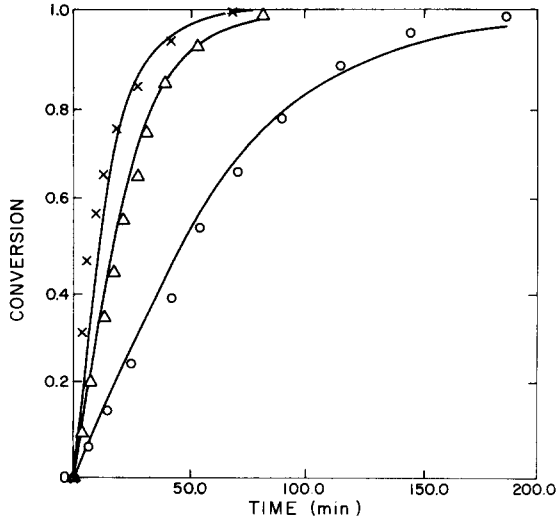

Figure 12 Conversion–time data and model predictions (———) for polymerizations under the following conditions: $[M] = 5.75\ mol\ l^{-1}$ of water, $[E] = 0.103\ mol\ l^{-1}$ of oil, $[AIBN] = 4.02\ mmol\ l^{-1}$ of oil, $\Phi_{w/o} = 1:1$, $N = 1000$ rpm; $T = 42.5$°C (○), 47°C (△) and 54°C (×)

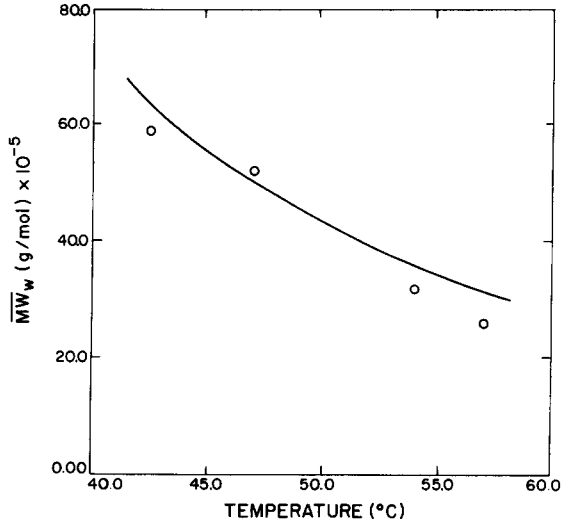

Figure 13 Final weight-average molecular weight ($\overline{MW}_w$) data and model predictions (○) as a function of temperature. Other reaction conditions were the same as in *Figure 12*

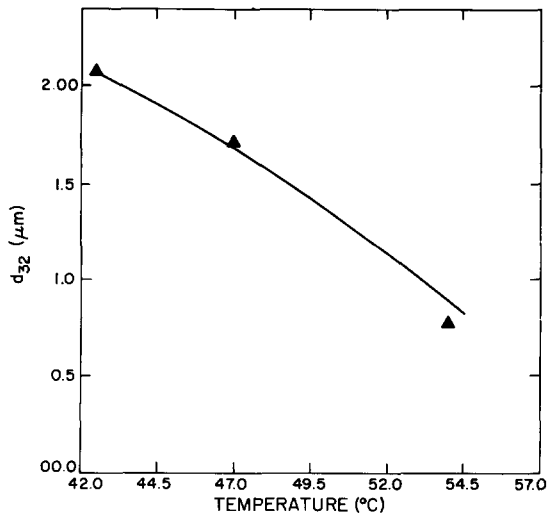

Figure 14 Volume-to-surface average particle diameter (d_{32}) as a function of reaction temperature. Other experimental conditions were the same as in *Figure 12*

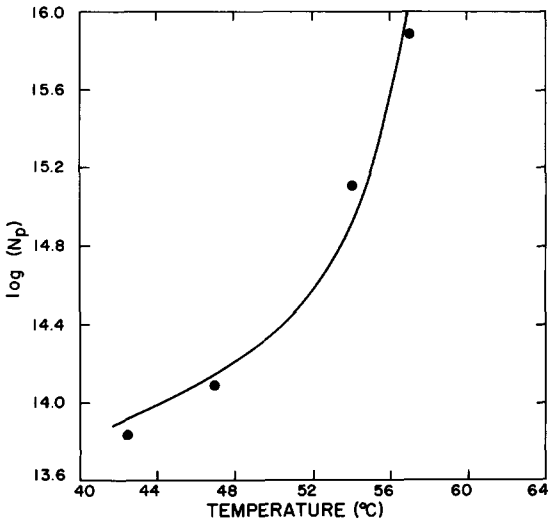

Figure 15 Experimentally measured number of particles per litre of continuous-phase (N_p) and model predictions (———) at several reaction temperatures. Other experimental conditions were the same as in *Figure 12*

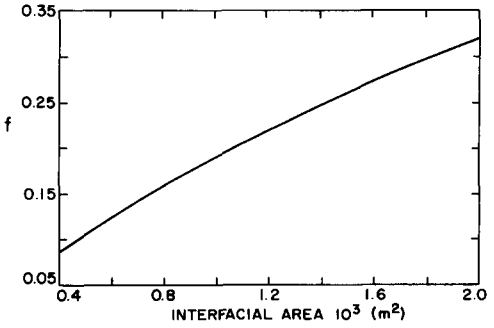

Figure 16 Efficiency of initiation of primary radicals (f) as a function of interfacial area. Other conditions of the simulations were: $T = 47°C$, [M] = 5.75 mol l^{-1} of water, [AIBN] = 4.02 mmol l^{-1} of oil, $\Phi_{w/o} = 1:1$

radicals per particle is significantly reduced because of the large increase in the number of particles per unit volume.

The rise in $\bar{n}$ with conversion is evidence of diffusion-controlled termination, which causes the total macroradical concentration to rise. The extent of diffusion-controlled termination in inverse microsuspension is similar in magnitude to solution acrylamide polymerizations, as is shown in *Figure 18*.

Effect of emulsifier type and concentration

Increasing the bulk level of emulsifier will cause both the interfacial and organic-phase concentrations to rise. The first effect lowers the surface tension, which produces smaller particles (*Figure 19*) and a slightly faster rate. However, these surface effects are small relative to the decrease in rate caused by the consumption of primary radicals and oligoradicals due to the additional soluble emulsifier (*Figure 20*). This, coupled with the very strong transfer to monomer reaction, implies that molecular weights should be fairly insensitive to the level of emulsifier. This is verified experimentally (*Figure 21*) over a broad range of SMO concentrations. The high measured molecular weight at the largest emulsifier level is believed to be an experimental anomaly.

The effect of different emulsifiers on rate has been discussed in the last section. *Figure 22* shows good agreement between the model and experimental data for both SMO and SMS.

The model can be applied to other types of emulsifiers or mixtures with co-surfactants, provided the transfer activity and the influence on interfacial tension are known.

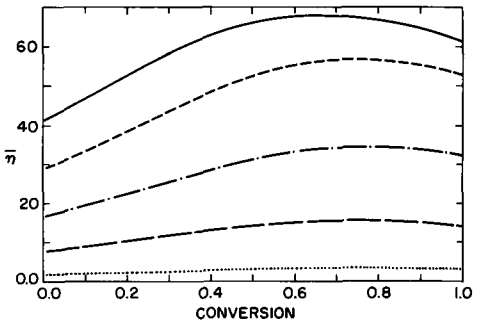

Figure 17 Average number of radicals per particle ($\bar{n}$) as a function of conversion for several reaction temperatures: 45°C (———), 50°C (– – –), 53°C (– · – · –), 55°C (— —) and 60°C (· · · · ·). Other conditions of the simulations were: [M] = 5.75 mol l^{-1} of water, [E] = 0.103 mol l^{-1} of oil, [AIBN] = 4.02 mmol l^{-1} of oil, $\Phi_{w/o} = 1:1$, $N = 1000$ rpm

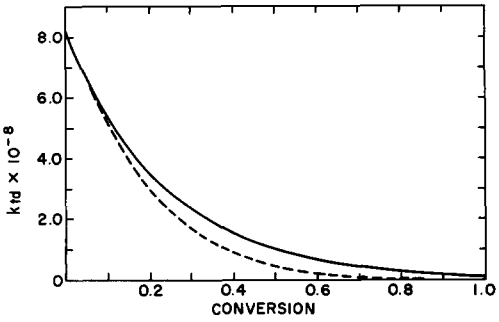

Figure 18 Extent of diffusion-controlled termination for inverse-microsuspension (——) and solution (– – –) polymerizations of acrylamide at 47°C. The gel effect was modelled using the empirical equation $k_{td}/k_{td}^0 = \exp(Aw_p)$, where w_p is the weight fraction of polymer in the aqueous phase and A is a constant determined from experimental data

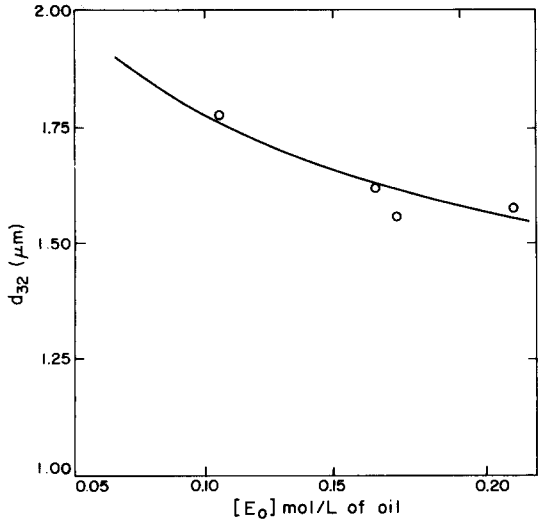

Figure 19 Volume-to-surface average particle size (d_{32}) data and model predictions (———) as a function of bulk emulsifier concentration. Other reaction conditions were: $T = 47°C$, [M] = 5.75 mol l^{-1} of water, [AIBN] = 4.02 mmol l^{-1} of oil, $\Phi_{w/o} = 1:1$, $N = 1000$ rpm

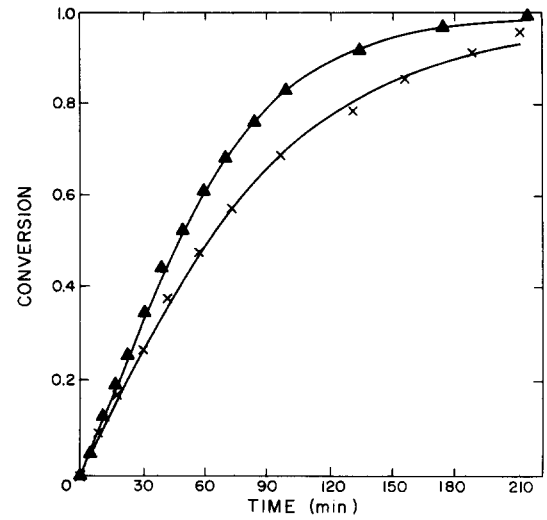

Figure 20 Conversion–time data and model predictions (———) for polymerizations with sorbitan monooleate at various concentrations: 0.103 (▲) and 0.211 (×) mol l^{-1} of oil. Other conditions were the same as *Figure 19*

Effect of phase ratio on rate

The reciprocal relationship between rate of polymerization and the phase ratio of water to oil (equation (10)) is surprising since it would be expected that, as the volume of the continuous phase is reduced, the consumption of primary radicals by reactions with emulsifier and hydrocarbons decreases. However, this effect is negligible compared to the reduction in turbulent intensity caused by the higher hold-ups. This produces larger particles and smaller interfacial areas, which reduce the radical capture efficiency and the rate.

Effect of the rate of agitation

The role of agitation is to maintain a stable emulsion throughout the polymerization. As the power input from the impeller increases, the droplets, which are produced by mechanical agitation and not homogeneous nucleation or micellar growth, become smaller (*Figure 23*). This increases the interfacial area and the rate (*Figure 24*).

At very low rates of agitation ($\leqslant 500$ rpm) the power input is insufficient to maintain emulsification and the kinetic model cannot be applied. This is also true at low emulsifier levels ($\leqslant 0.04$–0.06 mol l^{-1}).

The model gives good agreement with experimental data at various monomer concentrations up to 50 wt% (*Figure 25*).

Production of very-high-molecular-weight polymers

Under normal polymerization conditions high-molecular-weight products are obtained by lowering the temperature and initiator concentration. In inverse microsuspension, molecular weights can also be raised by increasing the level of double bonds in the polymer backbone. This can be accomplished by proper selection

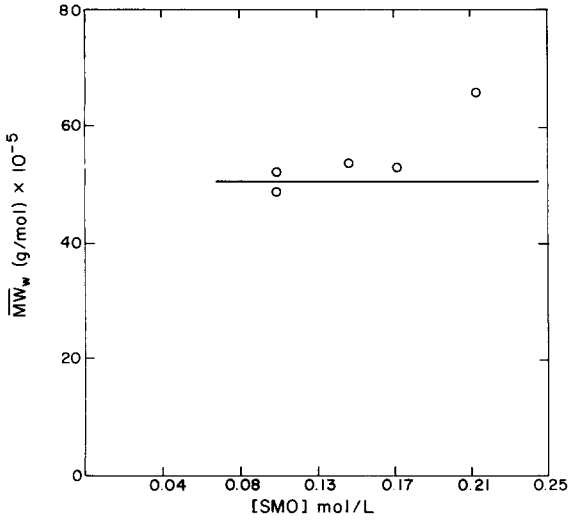

Figure 21 Final weight-average molecular weight ($\overline{MW}_w$) data and model predictions (———) for polymerizations with various concentrations of sorbitan monooleate. Other reaction conditions were the same as in *Figure 19*

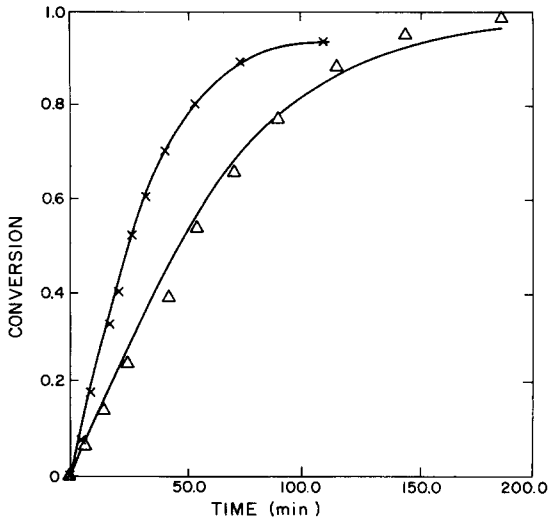

Figure 22 Conversion–time data and model predictions (———) for polymerizations with sorbitan monooleate (△) and sorbitan monostearate (×). The reaction conditions were: $T = 47°C$, [M] = 5.75 mol l^{-1} of water, [AIBN] = 4.02 mmol l^{-1} of oil, [E] = 0.103 mol l^{-1} of oil, $\Phi_{w/o} = 1:1$, $N = 1000$ rpm

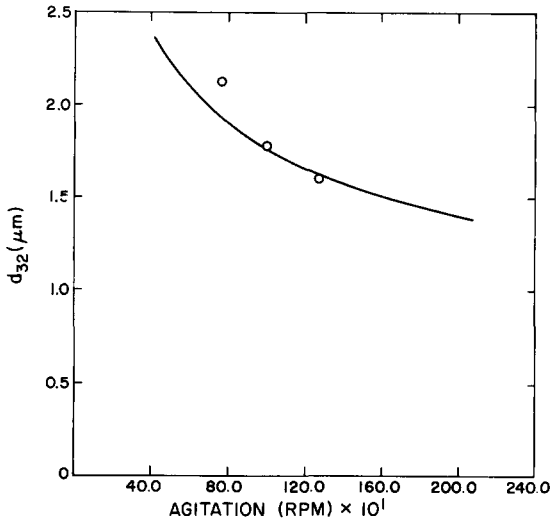

Figure 23 Experimentally measured volume-to-surface average particle diameter (d_{32}) and model predictions (———) as a function of the rate of agitation. Other reaction conditions were: $T=47°C$, $[M]=5.75\,mol\,l^{-1}$ of water, $[E]=0.103\,mol\,l^{-1}$ of oil, $[AIBN]=4.02\,mmol\,l^{-1}$ of oil, $\Phi_{w/o}=1:1$

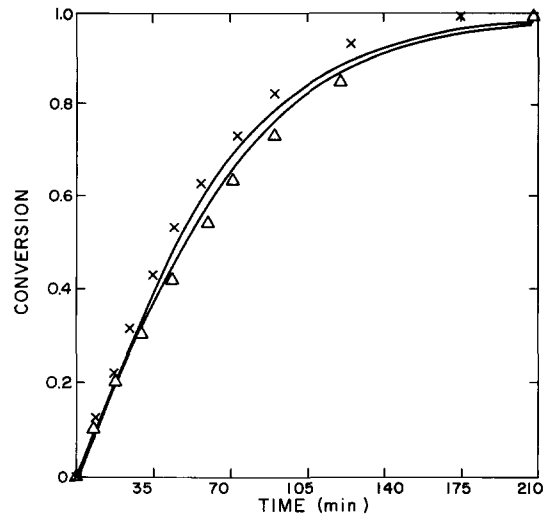

Figure 24 Conversion–time data and model predictions (———) as a function of the rate of agitation: 1000 rpm (△) and 1270 rpm (×). Other experimental conditions were the same as *Figure 23*

of the emulsifier where suitable emulsifiers would contain an extractable hydrogen in the hydrophilic end, and an accessible reactive carbon–carbon double bond. The presence of multiple double bonds may improve the branching probability and further increase molecular weights. In addition, suitable emulsifiers will also have to form a rigid interface that offers good stability for long periods, and lower the surface tension with moderate dosages.

In co-surfactant systems where several interfacial components are present, some species can be used to confer stability and others to provide sources of unsaturation.

Extension of the mechanism to include copolymerizations and the role of oxygen

The fundamental features of the mechanism are unchanged for homo- and copolymerizations. Additional reactions are, however, required to account for the difference in reactivity between the two types of monomers and macroradicals. If electrolytes are used, the influence of pH and salt level on the rate constants and dissociation equilibrium must also be known.

The addition of oxygen to control the polymerization rate is common industrially. Upon addition to an inverse microsuspension the oxygen diffuses into the oil and aqueous phases and consumes primary radicals. This can be modelled by adding the following steps to the kinetic mechanism:

$$O_{2(g)} \overset{\Phi_{O_2,1}}{\rightleftharpoons} O_{2(o)}$$

$$O_{2,o} + R^{\bullet}_{in,o} \xrightarrow{k_3} \text{inert products}$$

$$O_{2(o)} \overset{\Phi_{O_2,2}}{\rightleftharpoons} O_{2(w)}$$

$$O_{2,w} + R^{\bullet}_{in,w} \xrightarrow{k_3} \text{inert products}$$

where $\Phi_{O_2,1}$ and $\Phi_{O_2,2}$ are the partition coefficients of oxygen between the gas and oil, and between the oil and water phases, respectively. The subscripts, g, o and w designate gas-, organic- and water-phase concentrations. Knowledge of these partition coefficients and rate constants allows us to quantify the effect of an air pulse on rate.

The presence of excess oxygen may also reduce the molecular weight of the polymer by reacting with macroradicals. These polyoxyradicals have been postulated to propagate with monomer[50,51], generating a backbone that contains a weak O–O bond. This would be susceptible to scission at the elevated temperatures used at the end of commercial polymerizations.

Research on the effect of oxygen and the copolymerization of acrylamide with three cationic comonomers, diallyldimethylammonium chloride, dimethylaminoethyl methacrylate and dimethylaminoethyl acrylate, are presently in progress in our laboratories.

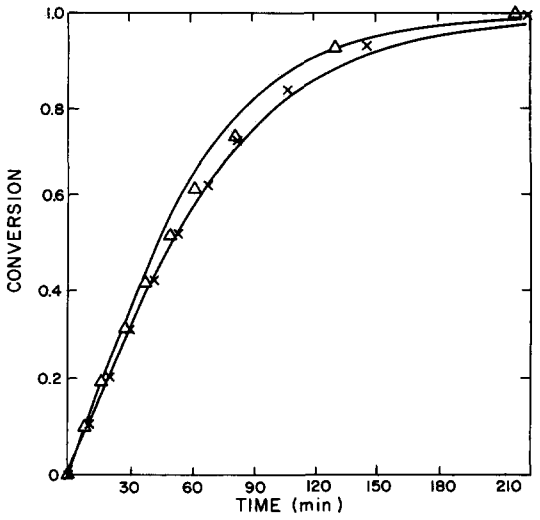

Figure 25 Conversion–time data and model predictions (———) for various monomer concentrations: 4.23 (×) and 7.04 (△) $mol\,l^{-1}$ of water. Other reaction conditions were: $T=47°C$, $[E]=0.103\,mol\,l^{-1}$ of oil, $[AIBN]=4.02\,mmol\,l^{-1}$ of oil, $\Phi_{w/o}=1:1$, $N=1000$ rpm

RECOMMENDATIONS FOR FUTURE WORK

Given the reasonably large body of kinetic data for heterophase polymerizations of acrylamide, additional investigations of the polymerization rate under various conditions are somewhat less important than improving our microscopic understanding of the process. This would include measurements of emulsifier partitioning between the continuous phase and the water–oil interface at various temperatures and ^{13}C n.m.r. confirmation of the role of emulsifier and oxygen on the polymerization.

The understanding of molecular weights would be improved by measurements by an absolute technique such as wide-angle light scattering or by utilizing recent advances in LALLS measurements of acrylamide which have reduced the error in molecular-weight measurements to less than 5%[52].

CONCLUSIONS

A mechanistic model has been developed for inverse-microsuspension polymerization and was found to predict conversion, molecular weight, particle size and number very well for acrylamide polymerizations at various levels of initiator, monomer, emulsifier, temperature and rate of agitation and for different types of initiators and emulsifiers. The mechanism can be characterized as a free-radical polymerization where unimolecular termination with interfacial emulsifier is dominant and mass transfer of primary radicals and oligoradicals is important.

The selection of emulsifier has been shown to be critical in the production of high-molecular-weight polymers, where the emulsifier is able to introduce carbon–carbon double bonds into the polymer backbone which can polymerize to form long-chain branches. This has implications not only for inverse microsuspension but for any heterophase water-in-oil polymerization. For example, in inverse-microemulsion polymerization[53], high levels (>20% by weight) of sorbitan emulsifiers are used and very small particle sizes ($\simeq$50 nm) are obtained. In such systems the reaction with interfacial emulsifier will be extremely important, due to the high surface-to-volume drop ratio, and will account for the measured high molecular weights.

ACKNOWLEDGEMENTS

We would like to thank the Natural Sciences and Engineering Council of Canada for financial support.

NOMENCLATURE

A	a parameter used in diffusion-controlled termination
A_E	total area occupied by emulsifier (m^2)
A_T	total interfacial area (m^2)
a_{sp}	specific interfacial area per litre of oil ($m^2\,l^{-1}$)
d_{32}	volume-to-surface average particle diameter (m)
d_p	particle diameter (m)
d_v	volume average particle diameter (m)
D	impeller diameter (m)
E	emulsifier
f	efficiency of initiation of primary radicals
f_e	efficiency of initiation of emulsifier radicals
HC	hydrocarbon
HC_{imp}	hydrocarbon-phase impurities
I	initiator
	Rate constants (units $l\,mol^{-1}\,min^{-1}$ unless otherwise specified)
k_1	reaction between macroradicals and hydrocarbon
k_2	reaction between macroradicals and oxygen in the oil phase
k_3	reaction between macroradicals and oxygen in the water phase
k_4	reaction between macroradicals and emulsifier in the oil phase
k_5	reaction between emulsifier radicals and hydrocarbon impurities
k_d	decomposition of initiator (min^{-1})
k_{fe}	transfer to emulsifier ($m^2\,mol^{-1}\,min^{-1}$)
k_{fm}	transfer to monomer
k_p	propagation
k_r, $k_{r,r}$	mass transfer coefficient of radicals: primary, length r ($m^3\,min^{-1}$)
k_r^*	$=k_r/A_T$ ($m\,min^{-1}$)
k_{td}	disproportionation termination
k^*	reaction with terminal double bonds
K	emulsifier equilibrium constant ($l\,m^{-2}$)
M	monomer
$\bar{M}_n$	number-average molecular weight ($g\,mol^{-1}$)
$\bar{M}_w$	weight-average molecular weight ($g\,mol^{-1}$)
M_m	molecular weight of monomer ($g\,mol^{-1}$)
MW_e	molecular weight of emulsifier ($g\,mol^{-1}$)
N	rate of agitation (rps)
N_A	Avogadro's number
N_E, $N_{E,o}$	moles of emulsifier: total, in oil phase
$\bar{n}$	average number of radicals per particle
N_p	number of polymer particles per litre of oil
O_2	oxygen
P_r	dead polymer chain of length r
Q_0, Q_1, Q_2	zero, first and second moments of the dead polymer distribution which do not contain terminal double bonds
$''Q_0$, $''Q_1$, $''Q_2$	moments of dead polymer distribution (polymers with terminal emulsifier double bonds)
Q_{0T}, Q_{1T}, Q_{2T}	total moments of dead polymer distribution
$R_{in}^{\bullet}$	initiator (primary) radical
$R_r^{\bullet}$, $R^{\bullet}$	macroradicals: length r, total sum of all lengths
$''R_r^{\bullet}$, $''R^{\bullet}$	macroradicals with terminal emulsifier double bonds: length r, total
$R_T^{\bullet}$	total macroradical concentration
R_p	rate of polymerization ($mol\,l^{-1}\,min^{-1}$)
V_o, V_w	volume of oil and water phases (l)
v, v_m	volume of surface emulsifier; volume of one complete monolayer (l)
W_e	Weber number (dimensionless)
w_p	weight fraction of polymer in aqueous phase
Y_0, Y_1, Y_2	zero, first and second moments of the macroradical distribution for macroradicals without terminal emulsifier double bonds
$''Y_0$, $''Y_1$, $''Y_2$	moments of macroradical distribution (macroradicals with terminal emulsifier double bonds)
Y_{0T}, Y_{1T}, Y_{2T}	total moments of macroradical distribution

α_s, α_v	surface and volume shape factors
Γ_E	interfacial emulsifier concentration (mol m^{-2})
ρ, ρ_E	density of continuous phase and emulsifier ($g\,l^{-1}$)
σ	surface tension ($N\,m^{-1}$)
Φ, $\Phi_{w/o}$	hold-up; phase ratio of water to oil
Φ_{m,r,O_2}	partition coefficient between oil and water: monomer, radicals, oxygen
g	gas-phase species
o	oil-phase species
r	polymer or macroradical of length r
w	water-phase species
bl	species in the boundary layer
•	designates a radical
"	species with a terminal emulsifier double bond
0	initial value
[]	concentration ($mol\,l^{-1}$)

(System of units: in general, SI was used except for concentrations, where l or dm^3 was used instead of m^3, and minutes were used in place of seconds)

REFERENCES

1 Cavell, E. A. S. *Makromol. Chem.* 1972, **54**, 70
2 Collinson, E., Dainton, F. S. and McNaughton, G. S. *Trans. Faraday Soc.* 1957, **53**, 476
3 Currie, D. J., Dainton, F. S. and Watt, W. S. *Polymer* 1965, **6**, 451
4 Friend, J. P. and Alexander, A. E. *J. Polym. Sci. (A-1)* 1968, **6**, 1833
5 Hamielec, A. E., Ishigie, T. and Lee, S.-I. *J. Appl. Polym. Sci.* 1971, **15**, 1607
6 Kim, C. J. and Hamielec, A. E. *Polymer* 1984, **25**, 845
7 Misra, G. S. and Rebello, J. J. *Makromol. Chem.* 1974, **175**, 3117
8 Pohl, K. and Rodriguez, F. *J. Appl. Polym. Sci.* 1980, **26**, 611
9 Riggs, J. P. and Rodriguez, F. *J. Polym. Sci. (A-1)* 1967, **5**, 3151
10 Suen, T. J., Schillier, A. M. and Russell, W. N. *Adv. Chem. Ser.* 1960, **17**, 217
11 Trubitsyna, S. N., Ismailov, I. and Askarov, M. A. *Vysokomol. Soed. (A)* 1978, **20**(11), 2608
12 Gromov, V. F., Matveyeva, A. V., Khomikovskii, P. M. and Abin, A. D. *Vysokomol. Soed. (A)* 1967, **9**(7), 1444
13 Kurenkov, V. F. and Myagchenkov, V. A. *Eur. Polym. J.* 1980, **16**, 1229
14 Communal, J. P., Fritz, J. and Papillon, B., Ger. Offen. 1973, 2248715
15 Necl, J. and Boutin, J., Eur. Pat. Appl. 1981, 15155
16 Perricone, A. C. and Lucas, J. M., Ger. Offen. 1981, 3008660
17 Takada, K., Fusaka, T. and Suzuki, M., Jap. Pat. 1979, 79-155296
18 Beres, J., Olkowska, J., Zawadsi, M., Macrejewski, Z., Pyplawiec, W. and Powierza, W., Pol. Pat. 1979, 102482
19 Dimonie, M., Oprescu, C., Dimione, V., Hubeca, G., Hagiopol, C. and Munteanu, M., Rom. Pat. 1978, 67005
20 Tago, A., Kudomi, H. and Sato, S., Jap. Pat. 1978, 78-41386
21 Graillot, C., Pichot, C., Guyot, A. and El-Aasser, M. S. *J. Polym. Sci., Polym. Chem. Edn.* 1986, **24**, 427
22 Baade, W. and Reichert, K.-H. *Makromol. Chem., Rapid Commun.* 1986, **7**, 235
23 Candau, F., Leong, Y. S. and Fitch, R. M. *J. Polym. Sci., Polym. Chem. Edn.* 1985, **23**, 193
24 Vanderhoff, J. W., Disteffano, F. V., El-Aasser, M. S., O'Leary, R., Schoffer, O. M. and Visioli, D. L. *J. Disp. Sci. Tech.* 1984, **5**, 323
25 Vanderhoff, J. W., El-Aasser, M. S. and Visioli, D. L. *Polym. Mater. Sci.-Eng.* 1984, **51**, 258
26 Dimone, M. V., Boghina, C. M., Marinescu, N. N., Marinescu, M. M., Cincu, C. I. and Oprescu, C. G. *Eur. Polym. J.* 1982, **18**, 639
27 McKechnie, M. T., 'Conference on Emulsion Polymers', London, June 1982, Paper No. 3
28 Trubitsyna, S. N., Ismailov, K. and Askarov, M. A. *Vysokomol. Soed. (A)* 1978, **20**, 2608
29 Kurenov, V. F., Osipova, T. M., Kaznetsov, E. V. and Myagchenkov, V. A. *Vysokomol. Soed. (B)* 1978, **20**, 647
30 Hunkeler, D., Masters Transfer Report, Department of Chemical Engineering, McMaster University, 1985
31 Singh, P., Huang, P. C. and Reichert, K.-H., 'Polymer Reaction Engineering' (Eds. K.-H. Reichert and W. Geiseler), Basel, 1986
32 Baade, W., Ph.D. Thesis, Technical University of Berlin, 1986
33 Klein, J. and Conrad, K.-D. *Makromol. Chem.* 1980, **181**, 227
34 Baade, W., Hunkeler, D. and Hamielec, A. E. *J. Appl. Polym. Sci.* accepted
35 Glukhikh, V., Graillat, V. and Pichot, C. *J. Polym. Sci., Polym. Chem. Edn.* 1987, **25**, 1127
36 Stacey, K. A. 'Light Scattering in Physical Chemistry', CVI, Butterworths, London, 1956
37 Sprow, F. B. *Chem. Eng. Sci.* 1967, **22**, 435
38 Brown, D. E. and Pitt, K., 'Proc. Chemica '70', Melbourne and Sydney, August 1970
39 Calderbank, P. H. *Trans. IChE* 1958, **36**, 443
40 Mynek, Y. and Resnick, W. *AIChE J.* 1972, **18**, 122
41 Caulalogou, C. A. and Tavlarides, L. L. *AIChE J.* 1976, **22**, 289
42 Vermeulen, T. G., Williams, G. M. and Langlois, G. E. *Chem. Eng. Prog.* 1955, **2**, 85F
43 Lee, J. C. and Tasakorn, P., 'Proc. Third European Conference on Mixing', 4–6 April 1979, BHRA Fluid Engineering Publishers, Cranfield, UK
44 Woods, D. R., 'Surfaces, Colloids and Unit Operations', McMaster University, 1986
45 'Azo Polymerization Initiators', Wako Pure Chemical Industries Ltd, 1983
46 Overberger, C. G., O'Shaughnessy, M. T. and Shalit, H. *J. Am. Chem. Soc.* 1949, **71**, 2261
47 Ishige, T. and Hamielec, A. E. *J. Appl. Polym. Sci.* 1973, **17**, 1479
48 Dainton, F. S. and Tordoff, M. *Trans. Faraday Soc.* 1957, **53**, 499
49 Candau, F., '194th Meeting of the American Chemical Society, Macromolecular Secretariat', New Orleans, 30 Aug.–4 Sept. 1987; Candau, F., Leong, Y. S., Pouyet, G. and Candau, S. J. *J. Colloid Interface Sci.* 1984, **101**, 167
50 George, M. H. and Ghosh, A. *J. Polym. Sci., Polym. Chem. Edn.* 1978, **16**, 981
51 Ghosh, A. and George, M. H. *Polymer* 1978, **19**, 1057
52 Hunkeler, D. and Hamielec, A. E. *J. Appl. Polym. Sci.* 1988, **35**, 1603
53 Candau, F., Zekhnini, Z., Heatly, F. and Franta, E. *Colloid Polym. Sci.* 1986, **264**, 676